International Journal of Power Electronics and Drive System (IJPEDS)
Vol. 17, No. 1, March 2026, pp. 640~652
ISSN: 2088-8694, DOI: 10.11591/ijpeds.v17.i1.pp640-652

Grey wolf optimization approach to optimal backstepping control for buck converter output voltage regulation

Sana Mouslim[1,2], Belkasem Imodane[2], Imane Outana[1,2], M'hand Oubella[2], El Mahfoud Boulaoutaq[2], Mohamed Ajaamoum[2]
[1]Interdisciplinary Applied Research Laboratory (LIDRA), International University of Agadir-Universiapolis, Agadir, Morocco
[2]Laboratory of Engineering Sciences and Energy Management (LASIME), Ibn Zohr University, National School of Applied Sciences, Agadir, Morocco

Article Info

Article history:

Received Sep 4, 2025
Revised Jan 6, 2026
Accepted Feb 15, 2026

Keywords:

Backstepping
Buck converter
DSP
Experimental validation
Grey wolf optimization
MATLAB/Simulink

ABSTRACT

DC-DC converters are essential in regulating voltage levels within DC power systems, relying on high-efficiency electronic switching devices such as MOSFETs to ensure effective power conversion. Despite their widespread use, one of the major challenges encountered in practical implementations lies in accurately tuning controller parameters particularly for nonlinear approaches such as the Backstepping controller. While recent studies have demonstrated the effectiveness of particle swarm optimization (PSO) in enhancing Backstepping control performance, further improvements remain possible. In this work, we propose the grey wolf optimization (GWO) algorithm as an advanced and efficient technique for the optimal tuning of backstepping controller parameters. The goal is to minimize the voltage tracking error between the reference and the output of the DC-DC buck converter, ensuring enhanced dynamic response and stability. Additionally, the proposed control strategy has been experimentally implemented and validated in a photovoltaic context, demonstrating its practical relevance and strong potential for real-world energy conversion applications.

Corresponding Author:

Sana Mouslim
Interdisciplinary Applied Research Laboratory (LIDRA), International University of Agadir-Universiapolis
Bab Al Madina, Tilila District, Agadir 80000, Morocco
Email: sana.mouslim@uiz.ac.ma

1. INTRODUCTION

The increasing demand for energy across various voltage levels has significantly driven the advancement of power electronics, particularly DC-DC converters, which are widely used due to their compactness and high efficiency compared to linear regulators [1], [2]. These converters are key components in diverse engineering applications such as maximum power point tracking (MPPT), photovoltaic (PV) systems, battery charging, and voltage regulation [3]. Designing an effective control strategy for such systems requires a precise mathematical model that captures the relationship between system inputs, state variables, and outputs [1]. However, the inherent nonlinearity of DC-DC converters especially within PV systems poses challenges in ensuring stability. While linearization techniques are often employed to approximate system behavior [4], nonlinear control strategies such as backstepping and sliding mode control have demonstrated superior robustness and stability characteristics [5], albeit at the cost of increased steady-state error and chattering effects.

Moreover, conventional control approaches like PID and fuzzy logic controllers are often limited by their sensitivity to system disturbances, leading to undesired fluctuations in output power and degraded power quality [6], [7]. To overcome these limitations, this work proposes the use of the backstepping control

technique, originally introduced by Krstić *et al.* [8] in 1991, to regulate the output voltage of a buck converter. Since the performance of the backstepping controller is highly dependent on the tuning of its internal parameters, modern metaheuristic optimization techniques such as particle swarm optimization (PSO) and genetic algorithms (GA) have been employed in prior studies [8], [9]. In this paper, the grey wolf optimizer (GWO) a nature-inspired algorithm based on the social hierarchy and hunting behavior of grey wolves [10] is applied to optimally tune the parameters of the backstepping controller. This study focuses on developing a comprehensive model and appropriately sizing the parameters of a buck converter operating in continuous conduction mode (CCM), taking into account fluctuations in both input voltage and load conditions. The converter model is established using the state-space averaging (SSA) approach within the MATLAB/Simulink environment. To achieve accurate voltage regulation, a backstepping control law is implemented, and its parameters are optimized through the grey wolf optimization (GWO) algorithm. Recent research has shown that GWO outperforms particle swarm optimization (PSO) and genetic algorithms (GA) when tuning controllers for DC-DC converters in photovoltaic (PV) systems, due to its effective exploration strategy and faster convergence. For example, a comparative study by Baraean *et al.* [11] demonstrated that controllers based on GWO deliver higher efficiency and enhanced stability in PV applications compared to PSO- and GA-based designs. Similarly, Krishnaram *et al.* [12] reported that GWO maintains robustness under dynamic environmental changes, improving voltage regulation in PV systems. These results highlight the potential of GWO to enhance both the performance and reliability of DC-DC converters in PV applications. Moreover, the proposed converter and GWO-based controller are validated experimentally. The structure of this paper is organized as follows: Section 2 presents the modeling and parameter sizing of the buck converter; Section 3 describes the backstepping controller and its implementation; Section 4 explains the integration of GWO for parameter optimization; subsequent sections detail simulation and experimental results, followed by performance evaluation and concluding remarks.

2. MODELLING AND DESIGN OF BUCK CONVERTER

Renowned for its simplicity and extensive use in power regulation, the buck converter is widely employed in power electronics applications. Its primary function is to reduce a higher input voltage to a desired lower output voltage while maintaining efficient energy conversion. The basic schematic of a buck converter with a resistive load is presented in Figure 1 [14], illustrating its fundamental components and operating structure.

2.1. The operating modes of the buck converter

The buck converter can operate in two distinct modes: continuous conduction mode (CCM) and discontinuous conduction mode (DCM). In this work, the focus is on modeling and parameter sizing of the buck converter in CCM. In this mode, the converter alternates between only two switching states: "S on, D off" and "S off, D on." Moreover, the inductor current never reaches zero [15]. Consequently, the analysis considers the converter in these two switching conditions. Such circuits are commonly referred to as series converters, as the energy flows directly from the source to the load.

Figure 2 shows the operation of switch S, during which the source energy is delivered to the load while also being stored in the inductor [16]. When the switch is turned off, the diode allows the inductor to release its stored energy. Figure 3 illustrates the buck converter circuit when switch S1 is in the open state [17], [18].

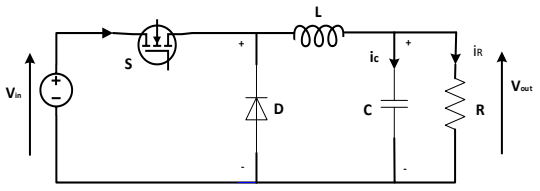

Figure 1. Buck converter

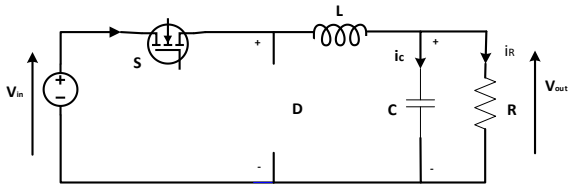

Figure 2. Buck converter when S_1 is closed

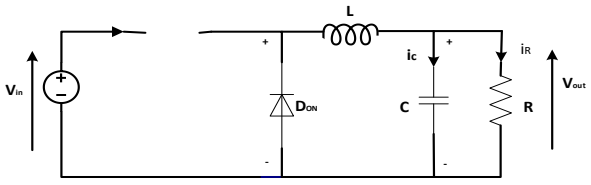

Figure 3. Buck converter when S_1 is open

2.2. State space modelling of DC-DC buck converter

This section introduces the state-space averaging (SSA) technique to mathematically represent the DC-DC converter under various operating conditions in continuous conduction mode. By applying Kirchhoff's Voltage Law (KVL) and Kirchhoff's Current Law (KCL), the differential equations describing the converter's state variables during the ON state of MOSFET S1 are derived as (1) [19].

$$\begin{cases} \frac{di_L}{dt} = \frac{V_{in}-V_c}{L} \\ \frac{dV_c}{dt} = \frac{i_L}{C} - \frac{V_c}{RC} \end{cases} \quad (1)$$

Similarly, for the OFF state of the switch, the representation in state space is transformed into (2) [20].

$$\begin{cases} \frac{di_L}{dt} = \frac{-V_c}{L} \\ \frac{dV_c}{dt} = \frac{i_L}{C} - \frac{V_c}{RC} \end{cases} \quad (2)$$

In matrix form, in (1) and (2) can be respectively shown as (3).

$$\begin{bmatrix} \frac{\mathrm{d}i_L}{\mathrm{dt}} \\ \frac{\mathrm{d}v_c}{\mathrm{dt}} \end{bmatrix} = \begin{bmatrix} 0 & \frac{-1}{L} \\ \frac{1}{C} & \frac{-1}{RC} \end{bmatrix} \begin{bmatrix} i_L \\ v_c \end{bmatrix} + \begin{bmatrix} \frac{1}{L} \\ 0 \end{bmatrix} V_{in} \quad (3)$$

$$\begin{bmatrix} \frac{\mathrm{d}i_L}{\mathrm{dt}} \\ \frac{\mathrm{d}v_c}{\mathrm{dt}} \end{bmatrix} = \begin{bmatrix} 0 & \frac{-1}{L} \\ \frac{1}{C} & \frac{-1}{RC} \end{bmatrix} \begin{bmatrix} i_L \\ v_c \end{bmatrix} + \begin{bmatrix} 0 \\ 0 \end{bmatrix} V_{in} \quad (4)$$

For each switching position, the system is linear; therefore, (3) and (4) are defined by state-space equations in the standard form as (5) and (6) [21].

$$\dot{\mathrm{X}} = A_1 X + B_1 u \quad (5)$$

$$\dot{\mathrm{X}} = A_2 X + B_2 u \quad (6)$$

Were, $X = [x_1 x_2]^T$.

The term x is the buck converter state vector defined as inductor current i_L and capacitor voltage v_C ,$\dot{x}$ it's derivative and u is the converter DC input vector. A_1, B_1 represent the status of input matrices for the switch ON state, and A_2, B_2 represent the status of input matrices for the switch OFF state. To represent the dynamic of the system and to find the averaged behavior of the buck converter over one switching period, the SSA method is used. By defining the duty cycle "d" as a weighting factor and using (3) and (4), the SSA equation in CCM is obtained:

$$\dot{\mathrm{X}} = AX + Bd \quad (7)$$

Where the complete state matrix is (8).

$$\mathrm{A}=\mathrm{A}_1\mathrm{d}+\mathrm{A}_2(1\text{-}\mathrm{d}) \quad (8)$$

$$\mathrm{B}=\mathrm{B}_1\mathrm{d}+\mathrm{B}_2(1\text{-}\mathrm{d}) \quad (9)$$

Hence, the dynamic equation of the system can be described by [1].

$$\begin{bmatrix} \frac{\mathrm{d}i_L}{\mathrm{dt}} \\ \frac{\mathrm{d}v_c}{\mathrm{dt}} \end{bmatrix} = \begin{bmatrix} 0 & \frac{1}{LR} - \frac{1}{L} \\ \frac{1}{C} & \frac{-1}{RC} \end{bmatrix} \begin{bmatrix} i_L \\ v_c \end{bmatrix} + \begin{bmatrix} \frac{V_{in}}{L} \\ 0 \end{bmatrix} \mathrm{d} \quad (10)$$

2.3. Designing of DC-DC buck converter parameters

Assuming the duty cycle of the buck converter operating in CCM is given by (11) [22].

$$d = \frac{V_{out}}{V_{in}} \quad (11)$$

The duty cycle varies depending on the applied input voltage in order to have a constant output voltage. For a buck converter, the ripple of the current in the inductance can be demonstrated by (12) [23].

$$\Delta I_L = d \times \frac{1-\mathrm{d}}{\mathrm{L\,f}} \times V_{in} \quad (12)$$

The ripple of the current is influenced by the frequency of the PWM signal, the duty cycle, and the L induction coefficient. So, the inductance value is calculated by (13) [24].

$$L_{min} = d \times \frac{1-\mathrm{d}}{\Delta I_L \,\mathrm{f}} \times V_{in} \quad (13)$$

And ripple in the output capacitor is considered to be 0.2% of the output voltage.

$$C = \frac{V_S \times (1-\mathrm{d})}{8 \times L \times f^2 \times \Delta V_{out}} \quad (14)$$

Employing Schottky diodes eliminates reverse recovery issues, which in turn reduces extra switching losses. The effective (RMS) current flowing through the diode is given by (15).

$$i_{d(eff)} = i_e \sqrt{(1-D)} \frac{i_s}{\sqrt{(1-D)}} \quad (15)$$

3. METHOD

3.1. Backstepping controller

Controllers based on the direct Lyapunov method offer a better alternative. The approach consists of finding a triplet (Lyapunov function, control law, adaptation law) that meets the specifications and takes into account the dynamics of the system [25]. Backstepping is the algorithm that has made this approach applicable to a large class of systems, independently of their order [26].

Step 1: The first error variable is defined by (16).

$$\varepsilon_1 = x_1 - V_{ref} \quad (16)$$

With these variables, the system (16) is written (17).

$$\dot{\varepsilon}_1 = \dot{x}_1 - \dot{V}_{ref} = \frac{x_2}{C} - \frac{x_1}{RC} - \dot{V}_{ref} \quad (17)$$

For such a system, the quadratic function V_1 is a good choice of the Lyapunov control function. Its derivative is given by (18).

$$V_1(\varepsilon_1) = \frac{1}{2}{\varepsilon_1}^2 \quad (18)$$

$$\dot{V}_1 = \varepsilon_1 \dot{\varepsilon}_1 = \varepsilon_1 \left(\frac{x_2}{C} - \frac{x_1}{RC} - \dot{V}_{ref} \right) \quad (19)$$

A judicious choice of x_2 would make $V_{1\cdot}$ negative and ensure the stability of the origin of the subsystem described by (19). Take as the value of x_2 the function α_1 such that and the derivative is written [27]:

$$\dot{V}_1 = -K_1 {\varepsilon_1}^2 \leq 0 \quad (20)$$

Hence, the asymptotic stability of the origin of (19).

$$\frac{x_2}{C} - \frac{x_1}{RC} - \dot{V}_{ref} = -K_1 \varepsilon_1 \quad (21)$$

Where $k_1 > 0$ is a design parameter. This gives in (22).

$$xd_2 = C\left(-K_1\varepsilon_1 + \dot{V}_{ref} + \frac{x_1}{RC}\right) \quad (22)$$

Step 2: We consider the subsystem (16), and we define the new error variable:

$$\varepsilon_2 = x_2 - xd_2 \quad (23)$$

Which represents the deviation between the state variable x_2 and its desired value α_1. Because x_2 cannot be forced to instantaneously take on a desired value, in this case, the error ε_2 is not, instantaneously, zero. The design in this step consists, then, in forcing it to cancel itself with a certain dynamic, chosen beforehand. For which we choose as the Lyapunov function [27]:

$$V_2(\varepsilon_1, \varepsilon_2) = \frac{1}{2}{\varepsilon_1}^2 + \frac{1}{2}{\varepsilon_2}^2 \quad (24)$$

The latter has the derivative (25).

$$\begin{aligned}\dot{V}_2 &= \varepsilon_1\dot{\varepsilon}_1 + \varepsilon_2\dot{\varepsilon}_2 \\ \dot{V}_2 &= \varepsilon_1\left[\left((\varepsilon_2 + xd_2)\frac{1}{C} - \frac{1}{RC}x_1 - \dot{V}_{ref}\right) + \left(\varepsilon_2 - \frac{1}{L}x_1 + \frac{V_e}{L}\beta - \dot{xd}_2\right)\right] \\ &= -K_1{\varepsilon_1}^2 + \varepsilon_2\left(\frac{1}{C}\varepsilon_1 - \frac{1}{L}x_1 + \frac{V_e}{L}\beta - \dot{xd}_2\right)\end{aligned} \quad (25)$$

Now we have the real u command, which is formulated as (26) and (27).

$$\frac{1}{C}\varepsilon_1 - \frac{1}{L}x_1 + \frac{V_e}{L}\beta - \dot{xd}_2 = -K_2\varepsilon_2 \quad (26)$$

$$\beta = \frac{L}{V_e}\left(-K_2\varepsilon_2 + \dot{xd}_2 + \frac{1}{L}x_1 - \frac{1}{C}\varepsilon_1\right) \quad (27)$$

Where $k_2 > 0$ is a second design parameter. With this choice, we have in (28).

$$\dot{V}_2 = -K_1{\varepsilon_1}^2 + -K_2{\varepsilon_2}^2 \quad (28)$$

3.2. Grey wolf optimizer

Grey wolves are classified as apex predators, occupying the top tier of the food chain. They usually form packs, with an average size of 5 to 12 members. Importantly, these packs maintain a strict dominance-based social hierarchy, as shown in Figure 4 [29]. From a mathematical perspective, the three best candidate solutions in the GWO algorithm are denoted as alpha (α), beta (β), and delta (δ). All other candidate solutions are classified as omega (ω). The search and hunting behavior in GWO is directed by the alpha, beta, and delta wolves, whereas the omega wolves adjust their positions by following these leading solutions. The pseudocode of the GWO algorithm is presented in Algorithm 1 [30].

Algorithm 1. Grey wolf optimization algorithm
Initialize the grey wolf population Xi, i=1,n
Initialize a, A and C
Calculate the fitness of each search agent
X_α = the best search agent
X_β = the second best search agent
X_δ = the third best search agent
while t<max number of iteration do
    for each search agent do
        Randomly initialize r_1 and r_2
        Update the position of the current search agent
    Update a,A and C
    Calculate the fitness of all search agents
    Update X_α,X_β and X_δ
    t = t + 1
return X_α

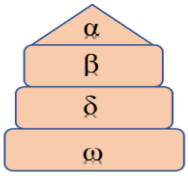

Figure 4. Hierarchy of the grey wolf (dominance decreases from top to bottom)

The pack's encircling behavior in hunting prey can be expressed as (29).

$$X(t+1) = X_p(t) - A * D \tag{29}$$

Where Xp is the position of the prey, A is the coefficient vector, and D is defined as follows:

$$D = \left|C * X_p(t) - X(t)\right| \tag{30}$$

Here, C represents the coefficient vector, X denotes the position of the grey wolf, and t is the current iteration number. The coefficient vectors $A$and $C$are calculated as follows:

$$A = 2a * r_1 - a, \tag{31}$$

$$C = 2\, r_2 \tag{32}$$

In this context, $r_1$and $r_2$are independent random numbers uniformly distributed between 0 and 1, and $a$denotes the encircling coefficient. Within the GWO algorithm, the coefficient a decreases linearly from 2 to 0, as given in (33).

$$a = 2 - 2(\frac{t}{T}) \tag{33}$$

Here, t represents the current iteration index, while T denotes the total number of iterations allowed. Within the GWO framework, the alpha (α), beta (β), and delta (δ) wolves are assumed to possess superior knowledge about the probable location of the prey. Consequently, these leading wolves direct the movement of the omega (ω) wolves toward the optimal solution. The position of each wolf is mathematically updated according to (34).

$$X(t+1) = \frac{X_1+X_2+X_3}{3} \tag{34}$$

Where X_1, X_2 et X_3 are calculated as (35)-(37).

$$X_1 = |X_\alpha - A_1 * D_\alpha| \tag{35}$$

$$X_2 = \left|X_\beta - A_2 * D_\beta\right| \tag{36}$$

$$X_3 = |X_\delta - A_3 * D_\delta| \tag{37}$$

Where X_α, X_β , et X_δ are the positions of alpha, beta, and delta at iteration t; and D_α, D_β, and D_δ are defined as in (38)-(40).

$$D_\alpha = |C_1 * X_\alpha - X| \tag{38}$$

$$D_\beta = \left|C_2 * X_\beta - X\right| \tag{39}$$

$$D_\delta = |C_3 * X_\delta - X| \tag{40}$$

Where C_1, C_2, et C_3 are calculated as in (32).

As shown in Figure 5, this section focuses on simulating the output voltage of the Buck converter using a backstepping controller enhanced through an optimization strategy. The grey wolf optimizer (GWO)

algorithm is employed to identify the optimal controller parameters. The optimization process involves iteratively evaluating the performance of the controller over a predetermined number of steps to determine the parameter set that yields the best results.

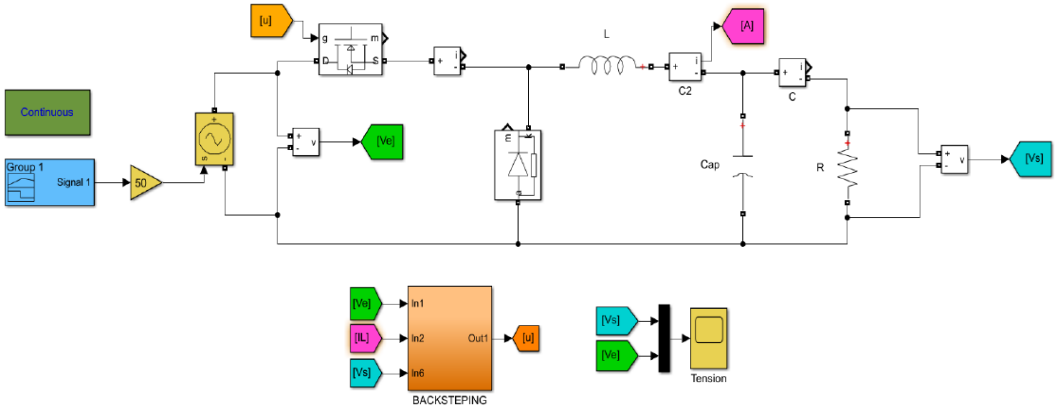

Figure 5. Overall view of the closed-loop system with the Backstepping controller

4. RESULTS AND DISCUSSION

4.1. Hardware section

In this section, we present an experimental platform, as illustrated in Figure 6, for the practical implementation of a DC-DC converter for a photovoltaic application. We will apply the backstepping control technique to regulate the converter's output voltage in order to power a resistive load. Based on the design of the buck converter developed in the second section, we were able to determine the normalized values of the converter components for the inductor L, capacitor C, and switching frequency f while optimizing them through practical tests after the converter design, as illustrated in Table 1.

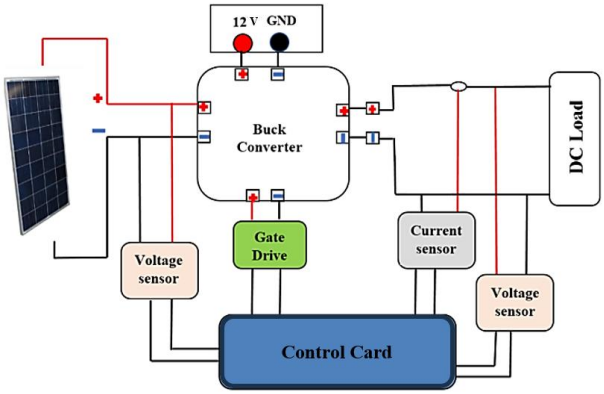

Figure 6. Overview of the proposed system

Table 1. Component values of the buck converter

Components	Values
L	120 uH
C	220 uF
R_1	10Ω
V_{ref}	12V
V_{in}	48V
f_s	40Khz
Mosfet	IRF520
Diode	MBR4045PT

The experimental setup, depicted in Figure 7, consists of a buck converter constructed with an IRF520 MOSFET, using the specified values for L and C. The output current of the converter is measured using an LTS 25-NP Hall effect sensor, while the output voltage (V_{out}) is monitored with an LV25-P sensor. The input voltage (V_{in}) can be adjusted as needed. The sensed current and voltage signals are sent to the signal conditioning board and then to the DSP's analog input channels. These feedback signals are used to regulate the reference voltage. The PWM signals generated by the DSP are routed through the PWM output, amplified via a driver circuit, and applied to the MOSFET gate.

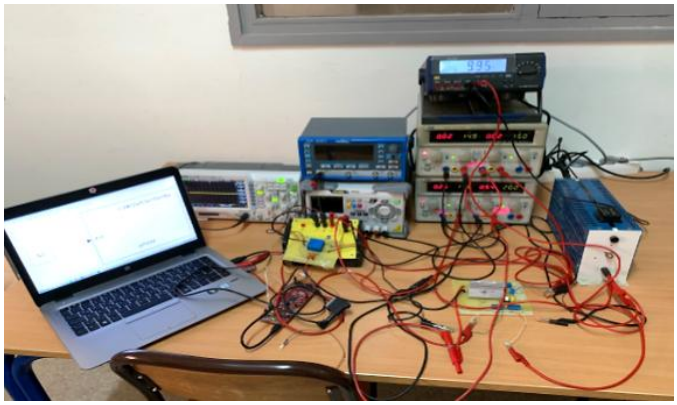

Figure 7. Overview of the proposed system

4.2. Simulation results

In this section, we aim to simulate the closed-loop system with the backstepping controller as shown in Figure 8, but without optimizing its parameters. In this simulation, the controller parameters will be randomly chosen without any prior optimization.

The results clearly show that the system fails to accurately track the desired reference voltage. Instead, significant overshoots and oscillations are observed in the system's response. These results highlight the importance of optimizing the parameters of the backstepping controller. By judiciously adjusting these parameters, it is possible to significantly improve the system's performance, reducing overshoots and ensuring a more stable and precise response to the reference voltage, as shown in Figure 9.

Figure 9 depicts the evolution of the output voltage of the buck converter with the backstepping controller optimized using the GWO algorithm. The results demonstrate a significant improvement compared to the previous simulation without optimization of the controller parameters. Optimizing the parameters of the backstepping controller using the GWO algorithm has enabled finding values that ensure a precise and fast system response. The optimal controller parameters have been adjusted to reduce tracking errors of the reference voltage, resulting in a response practically free from overshoots, as shown in Figure 10.

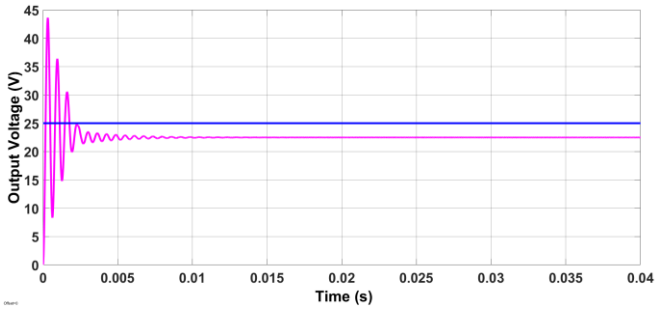

Figure 8. Output voltage V_{out} of buck converter with backstepping controller without optimization

To ensure the reliability and stability of the controller used in our buck converter, we conducted a study of the various disturbances that can affect its operation. To test the controller's robustness, we varied the input voltage and the load to assess its ability to maintain a constant output voltage (18 V) despite disturbances.

A well-designed and robust design will ensure consistent output voltage despite fluctuations to ensure stable voltage under variable conditions, we conducted a study of various scenarios for our buck converter, as depicted in Figure 10.

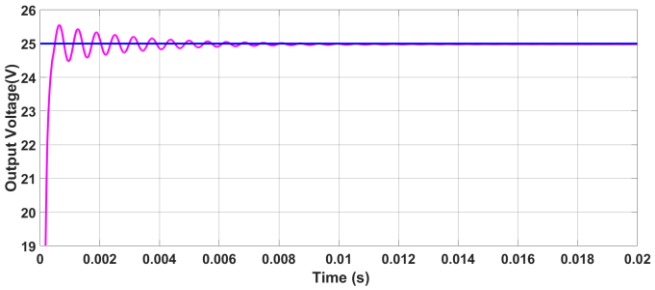

Figure 9. Output voltage V_{out} of buck converter with backstepping controller and with GW optimization

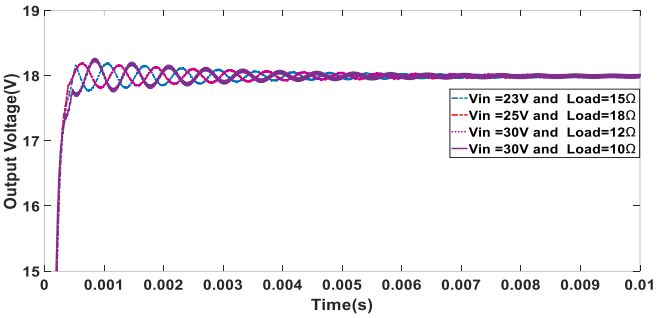

Figure 10. Output voltage for the buck converter with variable input voltage and variable load

4.3. Experimental results

The results of our study have shown a significant improvement in regulation performance using Backstepping with parameter optimization by the grey wolf algorithm (Figure 12). The regulation error has been significantly reduced, and the system has demonstrated a better ability to maintain a stable output voltage despite disturbances. During this experimental investigation, we implemented the PID control and evaluated its performance in terms of regulating the output voltage of the Buck converter in the presence of disturbances. Then, we introduced the SMC control, noting a significant improvement in regulation performance compared to PID control as shown in Table 2. However, we also noticed that tuning the parameters of the SMC control was delicate and required deep expertise.

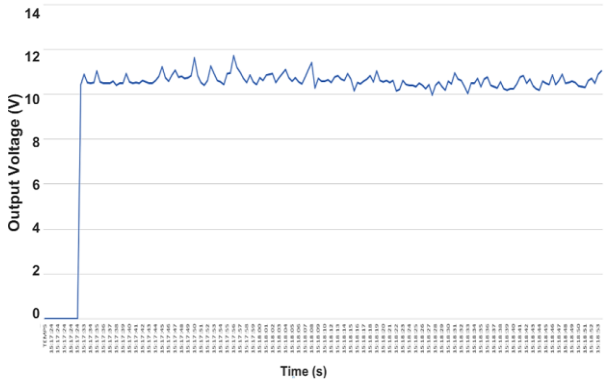

Figure 11. Experimental results of the buck converter output voltage with the backstepping controller without optimization

The comparative results presented in Table 2 clearly show that both SMC and Backstepping controllers outperform the conventional PID regulator in terms of dynamic response and voltage stability. While SMC significantly enhances performance by reducing the settling time and almost eliminating overshoot, the backstepping controller demonstrates the best overall behavior. It achieves the fastest settling time (1.97 s) and ensures the most stable voltage regulation with very narrow settling limits, confirming its superior ability to handle system nonlinearities. Despite a slightly higher overshoot than SMC, Backstepping maintains excellent damping characteristics and delivers a more precise and consistent control action, making it the most effective strategy among the three techniques.

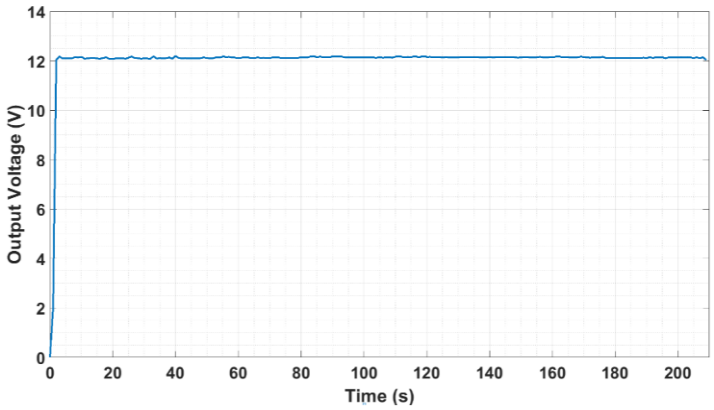

Figure 12. Experimental results of the buck converter output voltage with the backstepping controller with optimization

Table 2. Comparative analysis of the 3 control techniques

Controller	PID	SMC	Backstepping
Settling-time(s)	4.85	2.96	1.97
Settling-min(V)	11.67	11.92	12.03
Settling-max(V)	14.44	12.14	12.19
Overshoot (%)	20.32	1.21	1.65
Peak (V)	14.44	12.14	12.19

5. CONCLUSION

The research presented in this article has focused on the modeling and optimization of Backstepping control for regulating a static buck converter in renewable energy systems, particularly the photovoltaic (PV) solar energy conversion chain. It involves modeling non-isolated buck converters and designing Backstepping control to meet predefined conversion objectives. Additionally, it explores the use of optimization tools for optimal control of renewable energy conversion systems.

Our most notable contribution lies in the optimization of the backstepping control parameters using the GWO algorithm to regulate the buck converter. This approach stabilized the output voltage of the converter against disturbances in input voltage and load, thereby improving the robustness and performance of the photovoltaic system. Furthermore, we validated our optimized control approach by implementing an experimental platform consisting of a buck converter, a data acquisition card, and control based on the Texas Instruments TSM320F28335 DSP. The results of the experimental tests confirmed the effectiveness of our approach and its ability to operate in real-world conditions. As a future perspective, the GWO-optimized Backstepping control approach could be extended to more complex photovoltaic systems and evaluated under varying environmental conditions to better assess its robustness and real-time effectiveness.

ACKNOWLEDGMENTS

The authors would like to thank all individuals who provided technical support and valuable guidance during this work.

FUNDING INFORMATION

Authors state no funding involved.

AUTHOR CONTRIBUTIONS STATEMENT

This journal uses the Contributor Roles Taxonomy (CRediT) to recognize individual author contributions, reduce authorship disputes, and facilitate collaboration.

Name of Author	C	M	So	Va	Fo	I	R	D	O	E	Vi	Su	P	Fu
Sana Mouslim	✓	✓	✓	✓	✓	✓	✓	✓	✓	✓			✓	
Belkasem Imodane			✓	✓		✓	✓			✓	✓	✓		
Imane Outana		✓		✓			✓			✓	✓			
M'hand Oubella		✓	✓	✓			✓		✓			✓		
El Mahfoud Boulaoutaq	✓	✓		✓					✓		✓	✓		
Mohamed Ajaamoum						✓	✓		✓		✓	✓		

C : **C**onceptualization
M : **M**ethodology
So : **So**ftware
Va : **Va**lidation
Fo : **Fo**rmal analysis
I : **I**nvestigation
R : **R**esources
D : **D**ata Curation
O : Writing - **O**riginal Draft
E : Writing - Review & **E**diting
Vi : **Vi**sualization
Su : **Su**pervision
P : **P**roject administration
Fu : **Fu**nding acquisition

CONFLICT OF INTEREST STATEMENT

Authors state no conflict of interest.

DATA AVAILABILITY

The data that support the findings of this study are available from the corresponding author, upon reasonable request.

REFERENCES

[1] M. A. Alarcón-Carbajal, J. E. Carvajal-Rubio, J. D. Sánchez-Torres, D. E. Castro-Palazuelos, and G. J. Rubio-Astorga, "An Output Feedback Discrete-Time Controller for the DC-DC Buck Converter," *Energies*, vol. 15, no. 14, p. 5288, Jul. 2022, doi: 10.3390/en15145288.

[2] M. Bechouat, M. Sedraoui, Y. Soufi, L. Yousfi, A. Borni, and S. Kahla, "Particle swarm optimization backstepping controller for a grid-connected PV/wind hybrid system," *Journal of Engineering Science and Technology Review*, vol. 10, no. 1, pp. 91–99, 2017, doi: 10.25103/jestr.101.13.

[3] E. M. Boufounas, M. Hanine, A. El Amrani, and F. E. zahra Lamzouri, "Optimised backstepping sliding mode controller with integral action for MPPT-based photovoltaic system using PSO technique," *International Journal of Computer Aided Engineering and Technology*, vol. 18, no. 1/2/3, p. 97, 2023, doi: 10.1504/ijcaet.2023.10052476.

[4] T. Nabeshima, T. Sato, S. Yoshida, S. Chiba, and K. Onda, "Analysis and design considerations of a buck converter with a hysteretic PWM controller," *PESC Record - IEEE Annual Power Electronics Specialists Conference*, vol. 2, pp. 1711–1716, 2004, doi: 10.1109/pesc.2004.1355684.

[5] L. Liu, W. X. Zheng, and S. Ding, "An adaptive SOSM controller design by using a sliding-mode-based filter and its application to buck converter," *IEEE Transactions on Circuits and Systems I: Regular Papers*, vol. 67, no. 7, pp. 2409–2418, 2020, doi: 10.1109/TCSI.2020.2973254.

[6] K. Swathy, S. Jantre, Y. Jadhav, S. M. Labde, and P. Kadam, "Design and hardware implementation of closed loop buck converter using fuzzy logic controller," in *Proceedings of the 2nd International Conference on Electronics, Communication and Aerospace Technology, ICECA 2018*, 2018, pp. 175–180, doi: 10.1109/ICECA.2018.8474570.

[7] A. Humaidi and M. Hameed, "Development of a new adaptive backstepping control design for a non-strict and under-actuated system based on a PSO tuner," *Information (Switzerland)*, vol. 10, no. 2, 2019, doi: 10.3390/info10020038.

[8] M. Krstic, I. Kanellakopoulos, and P. V. Kokotovic, *Nonlinear and Adaptive Control Design*. New York, NY, USA: John Wiley & Sons, 1995.

[9] L. H. Abood, B. K. Oleiwi, and E. H. Ali, "Optimal backstepping controller for controlling DC motor speed," *Bulletin of Electrical Engineering and Informatics*, vol. 11, no. 5, pp. 2564–2572, 2022, doi: 10.11591/eei.v11i5.3940.

[10] O. Rodríguez-Abreo, F. J. Ornelas-Rodríguez, A. Ramírez-Pedraza, J. B. Hurtado-Ramos, and J. J. González-Barbosa, "Backstepping control for a UAV-manipulator tuned by Cuckoo Search algorithm," *Robotics and Autonomous Systems*, vol. 147, 2022, doi: 10.1016/j.robot.2021.103910.

[11] A. Baraean, W. M. Hamanah, A. Bawazir, S. Baraean, and M. A. Abido, "Optimal nonlinear backstepping controller design of a quadrotor-slung load system using particle swarm optimization," *Alexandria Engineering Journal*, vol. 68, pp. 551–560, 2023, doi: 10.1016/j.aej.2023.01.050.

[12] K. Krishnaram, T. Suresh Padmanabhan, F. Alsaif, and S. Senthilkumar, "Development of grey wolf optimization based modified fast terminal sliding mode controller for three phase interleaved boost converter fed PV system," *Scientific Reports*, vol. 14, no. 1, 2024, doi: 10.1038/s41598-024-59900-z.

[13] S. Chtita *et al.*, "A novel hybrid GWO–PSO-based maximum power point tracking for photovoltaic systems operating under partial shading conditions," *Scientific Reports*, vol. 12, no. 1, 2022, doi: 10.1038/s41598-022-14733-6.
[14] S. Zouga, M. Benchagra, and A. Abdallah, "Backstepping control based on the pso algorithm for a three-phase pv system connected to the grid under load variation," in *2020 International Conference on Electrical and Information Technologies, ICEIT 2020*, 2020 doi: 10.1109/ICEIT48248.2020.9113235.
[15] H. Sorouri, M. Sedighizadeh, A. Oshnoei, and R. Khezri, "An intelligent adaptive control of DC–DC power buck converters," *International Journal of Electrical Power & Energy Systems*, vol. 141, p. 108099, Oct. 2022, doi: 10.1016/j.ijepes.2022.108099.
[16] O. Boutebba, S. Semcheddine, F. Krim, B. Talbi, A. Reatti, and F. Corti, "Robust non-linear controller design for DC-DC buck converter via modified back-stepping methodology," *Elektronika ir Elektrotechnika*, vol. 28, no. 6, pp. 4–11, Dec. 2022, doi: 10.5755/j02.eie.31487.
[17] M. Salimi, J. Soltani, G. A. Markadeh, and N. R. Abjadi, "Indirect output voltage regulation of DC–DC buck/boost converter operating in continuous and discontinuous conduction modes using adaptive backstepping approach," *IET Power Electronics*, vol. 6, no. 4, pp. 732–741, Apr. 2013, doi: 10.1049/iet-pel.2012.0198.
[18] F. Khavari, S. M. Ghamari, M. Abdollahzadeh, and H. Mollaee, "Design of a novel robust type-2 fuzzy-based adaptive backstepping controller optimized with antlion algorithm for buck converter," *IET Control Theory & Applications*, vol. 17, no. 9, pp. 1132–1143, Jun. 2023, doi: 10.1049/cth2.12445.
[19] K. Prag, M. Woolway, and T. Celik, "Data-driven model predictive control of DC-to-DC buck-boost converter," *IEEE Access*, vol. 9, pp. 101902–101915, 2021, doi: 10.1109/ACCESS.2021.3098169.
[20] V. Du Phan, D. T. Duong, V. C. Le, and S. P. Ho, "An adaptive control strategy for DC/DC converters using command-filtered backstepping and disturbance rejection," *Micromachines*, vol. 16, no. 12, p. 1412, Dec. 2025, doi: 10.3390/mi16121412.
[21] X. Gong and J. Fei, "Adaptive Neural Backstepping Terminal Sliding Mode Control of a DC-DC Buck Converter," *Sensors*, vol. 23, no. 17, p. 7450, Aug. 2023, doi: 10.3390/s23177450.
[22] B. Vatankhah and M. Farrokhi, "Offset-free adaptive nonlinear model predictive control with disturbance observer for DC-DC buck converters," *Turkish Journal of Electrical Engineering & Computer Sciences*, vol. 25, pp. 2195–2206, 2017, doi: 10.3906/elk-1512-69.
[23] H. Sorouri, A. Oshnoei, M. Novak, F. Blaabjerg, and A. Anvari-Moghaddam, "Learning-based model predictive control of DC-DC buck converters in DC microgrids: A multi-agent deep reinforcement learning approach," *Energies*, vol. 15, no. 15, p. 5399, Jul. 2022, doi: 10.3390/en15155399.
[24] S. A. Saadat, S. M. Ghamari, and H. Mollaee, "Adaptive backstepping controller design on buck converter with a novel improved identification method," *IET Control Theory & Applications*, vol. 16, no. 5, pp. 485–495, Mar. 2022, doi: 10.1049/cth2.12241.
[25] H. S. Zad, A. Ulasyar, A. Zohaib, M. Irfan, S. A. Haider, and Z. Yaqoob, "Adaptive sliding mode control of DC–DC buck converter with load fluctuations for renewable energy systems," in *ICAME 2024*, Basel Switzerland: MDPI, Sep. 2024, p. 10. doi: 10.3390/engproc2024075010.
[26] P. Qiao and H. Sun, "Generalized proportional integral observer and Kalman-filter-based composite control for DC-DC buck converters," *Actuators*, vol. 12, no. 1, p. 20, Jan. 2023, doi: 10.3390/act12010020.
[27] J. Šimko, M. Praženica, R. Koňarik, S. Kaščák, and P. Klčo, "Output voltage control of a synchronous buck DC/DC converter using artificial neural networks," *Algorithms*, vol. 18, no. 9, p. 555, Sep. 2025, doi: 10.3390/a18090555.
[28] A. H. Mary, A. H. Miry, and M. H. Miry, "System uncertainties estimation based adaptive robust backstepping control for DC DC buck converter," *International Journal of Electrical and Computer Engineering (IJECE)*, vol. 11, no. 1, p. 347, Feb. 2021, doi: 10.11591/ijece.v11i1.pp347-355.
[29] O. Saleem, K. R. Ahmad, and J. Iqbal, "Fuzzy-augmented model reference adaptive PID control law design for robust voltage regulation in DC–DC buck converters," *Mathematics*, vol. 12, no. 12, p. 1893, Jun. 2024, doi: 10.3390/math12121893.
[30] S. Das Gangula, T. K. Nizami, and R. R. Udumula, "Experimental investigation on backstepping control of DC-DC buck converter fed constant power load," *IFAC-PapersOnLine*, vol. 57, pp. 137–142, 2024, doi: 10.1016/j.ifacol.2024.05.024.

BIOGRAPHIES OF AUTHORS

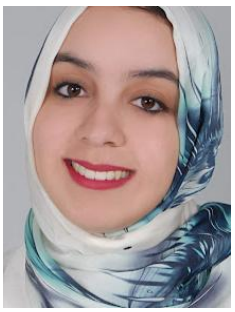

Sana Mouslim is a professor at the Polytechnic School of Agadir, Universiapolis – International University of Agadir, Morocco. She earned her Ph.D. in Electrical Engineering, specializing in Automation and Renewable Energy, from the National School of Applied Sciences (ENSA) of Agadir. Her research focuses on the control and optimization of DC-DC converters for photovoltaic applications, including the development of advanced control strategies to improve the performance and efficiency of power electronic systems. She is a member of two research laboratories: Laboratory of Engineering Sciences and Energy Management (LASIME) and Interdisciplinary Applied Research Laboratory (LIDRA), where she contributes to applied research in renewable energy and power. She can be contacted at email: sana.mouslim@uiz.ac.ma.

Belkasem Imodane is a Ph.D. student in electrical engineering at the University of Ibn Zohr, Agadir. He graduated as an embedded systems engineer in 2021 from the National School of Applied Sciences, Agadir, Morocco. Subsequently, he joined the research group at the Engineering Sciences and Energy Management Laboratory, University of Ibn Zohr, Agadir, Morocco. His research focuses on renewable energies for his doctoral thesis. He can be contacted at email: b.imodane@uiz.ac.ma.

Imane Outana holds a Ph.D. in Physics, specializing in energetic, from Abdelmalek Essaâdi University in Tétouan. She is currently an assistant professor and program coordinator at the Polytechnique School of Agadir, Universiapolis. Her research focuses on renewable energies, particularly photovoltaics, concentrated solar power (CSP), and wind energy. She is also engaged in the study of green hydrogen production, energy storage, and energy efficiency. She can be contacted at email: outana.imane@e-polytechnique.ma.

M'hand Oubella holds the position of professor in higher education at the High School of Technologies of Agadir (ESTA), Ibn Zohr University, Agadir, Morocco. He obtained his Ph.D. in energetic and process engineering from the National School of Applied Sciences (ENSA) of Agadir in 2014. Currently, he is a member of the Laboratory of Engineering Sciences and Energy Management (LASIME) at the High School of Technologies of Agadir (ESTA), and his research focuses on intelligent systems and energy management, with a particular emphasis on renewable energies. This research is conducted within the framework of the research team known as Intelligent Systems and Energy Management (ERSIME). He can be contacted at email: m.oubella@uiz.ac.ma.

El Mahfoud Boulaoutaq was born in the Agadir region in southern Morocco. His education focused on electrical engineering disciplines; bachelor's degree (1993), license (1997), aggregation diploma (2007), and master's degree (2017). Since 2018, he has been a Ph.D. student in the design of controllers for wind turbines connected to the distribution network. He can be contacted at email: elmahfoud.boulaoutaq@edu.uiz.ac.ma.

Mohamed Ajaamoum is a professor with a Ph.D. in the Department of Electrical Engineering, High School of Technology of Agadir, Ibn Zohr University, Agadir, Morocco. His research interests are in photovoltaic systems, fuzzy control, neural networks, renewable energy technologies, system modeling, and power electronics. He can be contacted at email: m.ajaamoum@uiz.ac.ma.